Molecular Therapy
Original Article

Development and Mechanism of Small Activating RNA Targeting CEBPA, a Novel Therapeutic in Clinical Trials for Liver Cancer

Jon Voutila,[1,7] Vikash Reebye,[2,7] Thomas C. Roberts,[3] Pantelitsa Protopapa,[1] Pinelopi Andrikakou,[2] David C. Blakey,[1] Robert Habib,[1] Hans Huber,[4] Pal Saetrom,[5] John J. Rossi,[6] and Nagy A. Habib[2]

[1]MiNA Therapeutics, Ltd., London, UK; [2]Department of Surgery and Cancer, Imperial College London, London, UK; [3]The Scripps Research Institute, San Diego, CA, USA; [4]BioTD Strategies, LLC, Philadelphia, PA, USA; [5]Department of Cancer Research and Molecular Medicine, Norwegian University of Science and Technology, Trondheim, Norway; [6]Department of Molecular and Cellular Biology, Beckman Research Institute of City of Hope, Duarte, CA, USA

Small activating RNAs (saRNAs) are short double-stranded oligonucleotides that selectively increase gene transcription. Here, we describe the development of an saRNA that upregulates the transcription factor CCATT/enhancer binding protein alpha (CEBPA), investigate its mode of action, and describe its development into a clinical candidate. A bioinformatically directed nucleotide walk around the CEBPA gene identified an saRNA sequence that upregulates CEBPA mRNA 2.5-fold in human hepatocellular carcinoma cells. A nuclear run-on assay confirmed that this upregulation is a transcriptionally driven process. Mechanistic experiments demonstrate that Argonaute-2 (Ago2) is required for saRNA activity, with the guide strand of the saRNA shown to be associated with Ago2 and localized at the CEBPA genomic locus using RNA chromatin immunoprecipitation (ChIP) assays. The data support a sequence-specific on-target saRNA activity that leads to enhanced CEBPA mRNA transcription. Chemical modifications were introduced in the saRNA duplex to prevent activation of the innate immunity. This modified saRNA retains activation of CEBPA mRNA and downstream targets and inhibits growth of liver cancer cell lines in vitro. This novel drug has been encapsulated in a liposomal formulation for liver delivery, is currently in a phase I clinical trial for patients with liver cancer, and represents the first human study of an saRNA therapeutic.

INTRODUCTION

RNA activation (RNAa) was first described in 2006, where it was reported that short double-stranded RNAs targeted to the promoter region of a gene can activate its transcription.[1] These small activating RNAs (saRNAs) have since been shown to activate a wide variety of genes in several mammalian species.[2–11] Although similar to RNA interference (RNAi) in that it is mediated by short RNAs and requires Argonaute-2 (Ago2), RNAa is distinct in its kinetics and ability to selectively induce transcriptional elongation of a target gene in the nucleus.[12] The further molecular mechanisms that distinguish RNAa from RNAi continue to be investigated, such as the identification of CTR9 and RHA as necessary cofactors for saRNA activity and the role of RNA polymerase II.[13] This technology provides a new research tool for selective gene activation, but also a novel therapeutic approach for diseases in which endogenous gene expression has been downregulated through mutation or transcriptional/translational repression.

Hepatocellular carcinoma (HCC) is most commonly caused by chronic liver damage due to cirrhosis from hepatitis virus infection, alcohol abuse, or non-alcoholic fatty liver disease.[14,15] Although surgical resection is the preferred treatment for HCC, only 10%–25% of tumors are resectable, with a 5-year recurrence rate of up to 80%.[16] The standard of care treatment for advanced HCC is the multikinase inhibitor sorafenib, which has a median survival increase of just 2.8 months and a less than 5% response rate.[17] There thus remains a critical unmet need for treatment of patients with HCC who are ineligible for tumor resection.

The CCAAT/enhancer-binding protein alpha (CEBPA) gene encodes C/EBP-α, a basic-leucine zipper class transcription factor that is critical for the differentiation and function of liver and adipose tissue as well as the myeloid lineage.[18] Deletion of the CEBPA gene in the liver results in dysregulation of liver-specific transcription factors and impaired hepatocyte maturation.[19] A rat model of HCC as well as a retrospective analysis of human HCC samples shows that C/EBP-α is downregulated in HCC and associated with poor survival.[20,21] This suggests that chronic liver disease leading to HCC may cause a dysregulation of the liver-specific transcriptional network, contributing to tumorigenesis or exacerbating the poor liver function seen in HCC.[22] C/EBP-α has also been

Received 23 February 2017; accepted 31 July 2017;
http://dx.doi.org/10.1016/j.ymthe.2017.07.018.

[7]These authors contributed equally to this work.

Correspondence: Jon Voutila, MiNA Therapeutics, Ltd., London, UK.
E-mail: jon@minatx.com
Correspondence: Nagy A. Habib, Department of Surgery and Cancer, Imperial College London, London, UK.
E-mail: nagy.habib@imperial.ac.uk

described as a tumor suppressor, leading to mitotic arrest through activation of p21 and repression of E2Fs and cyclin-dependent kinases (CDKs).[23] Indeed, CEBPA knock-in mice show partial protection from HCC,[24] showing that upregulation of C/EBP-α activity has a potential to not only improve liver function, but also limit HCC growth. Because impaired liver function is a common complication of HCC limiting the use of surgical resection,[25] activation of the C/EBP-α pathway is an attractive therapeutic target for saRNA, with the potential to improve normal liver function while inhibiting tumor growth.

We previously designed a CEBPA saRNA that showed increased expression of hepatocyte-specific factors, such as albumin, hepatocyte nuclear factor (HNF)4α, and HNF1α, and inhibited tumor growth in a rat model of HCC.[11] Here, we describe the development of this saRNA into a clinical candidate, and demonstrate that its activity is an on-target mechanism consistent with RNAa. The final saRNA, CEBPA-51, has been formulated in a NOV340 SMARTICLE (MTL-CEBPA) and is currently in phase I clinical trials for the improvement of liver function in patients with HCC.[26]

RESULTS

Our saRNA bioinformatics algorithm, described previously,[7] identified several hotspots of putative saRNA activity at the CEBPA gene locus. Two of these hotspots were within the coding region of CEBPA where a noncoding RNA (GenBank: AW665812) overlaps the gene in the antisense orientation relative to CEBPA mRNA (Figure 1A). We synthesized a series of saRNA oligonucleotides to perform a nucleotide walk across these two hotspots, called AW1 and AW2 (Table S1). These candidate CEBPA saRNAs were tested by transfection into the human HCC cell line HepG2, and their ability to upregulate CEBPA and C/EBP-α target gene albumin[18] mRNA was measured (Figures 1B and 1C). This screen identified 4 sequences that upregulated both CEBPA and albumin mRNA >1.5-fold. We chose the sequence AW1-51 for further development as a clinical candidate because it had the highest CEBPA mRNA upregulation (2.5-fold) and was in the same hotspot as our previously published CEBPA saRNA. Transfection of increasing concentrations of AW1-51 showed a clear dose response of CEBPA mRNA upregulation, with an EC_{50} of 5.36 nM under the conditions tested in this assay (Figure S1A). Under the same conditions, a CEBPA small interfering RNA (siRNA) had an IC_{50} of 0.05 nM (Figure S1B).

To test whether upregulation of CEBPA mRNA by AW1-51 led to an increase in functional C/EBP protein, we used a C/EBP luciferase reporter assay. Transfection of AW1-51 in HepG2 cells caused a significant increase in luciferase activity (Figure 2A), indicating an increase in functional C/EBP activity.

An increase in steady-state mRNA could be due to enhancing mRNA stability, whereas true saRNA activity requires activation of transcription of target gene mRNA. To determine if AW1-51 activates CEBPA transcription, we measured nascent CEBPA mRNA transcription in a nuclear run-on experiment. After transfection of AW1-51 in HepG2 cells, nascent CEBPA mRNA rose 3-fold compared to control transfected cells (Figure 2B), indicating activation of transcription.

To determine which strand of the AW1-51 duplex was responsible for saRNA activity, we used a 5′ inverted abasic modification on each strand individually to block strand loading into Ago2.[27] As expected, a 5′ inverted abasic modification on both strands completely negated saRNA activity, but when only the sense strand (SS) was modified, CEBPA mRNA was upregulated 2.5-fold (Figure 2C). This indicates that the antisense strand (AS) is the guide strand loaded into Ago2. We then sought to test if this is a true on-target mechanism by introducing mutations to the seed region of the saRNA. Introducing a single mutation into position 3 or 4 of the seed region reduced saRNA activity to below statistical significance, whereas additional mutations caused a complete loss of activity (Figure 2D). A duplex composed of the scrambled AW1-51 sequence was also not active (Figure 2D).

Because the AW1-51 AS is the guide strand loaded into Ago2, we wanted to rule out target cleavage of either non-coding RNA (ncRNA) GenBank: AW665812 or other off-target RNAs being responsible for the saRNA activity. When three mutations were introduced to the center of the AW1-51 sequence to prevent target cleavage,[28] there was no significant loss of saRNA activity measured by upregulation of CEBPA mRNA (Figure 2E). Further, strand-specific reverse transcription followed by qPCR with primers flanking the saRNA target site showed that GenBank: AW665812 RNA is upregulated rather than being downregulated by AW1-51 (Figure 2F), demonstrating that cleavage is not required for CEBPA upregulation.

To further develop AW1-51 as a clinical candidate saRNA, we tested different patterns of 2′-O-methyl base modifications to prevent immune stimulation (Figure S2A). We first tested to see if these modifications affected saRNA activity. As above, a 5′ SS inverted abasic on the SS sequence does not affect saRNA activity, and two different methylation patterns were well tolerated (Figure S2B). The lack of activity of modification pattern 3 suggests that modifications to the guide strand may not be well-tolerated. These two active modified AW1-51 saRNAs were tested for TLR activation by transfection into primary human PBMCs, and one of two patterns (modification pattern 2) showed negligible tumor necrosis factor alpha (TNF-α) and interferon α (IFNα) secretion in two donors (Figure S2C). This non-immunostimulatory-modified AW1-51 saRNA was named CEBPA-51.

We next assessed the activity of CEBPA-51 in the HCC lines HepG2 and Hep3B. Transfection of CEBPA-51 causes 1.5- to 2.5-fold upregulation of CEBPA mRNA (Figure 3A) and a corresponding increase in C/EBP-α protein (Figure 3B) by western blot, as well as a 1.5- to 2-fold upregulation of C/EBP-α downstream target albumin mRNA in both cell lines. The effect of CEBPA-51 on HCC cell proliferation was tested by a water-soluble tetrazolium salt (WST-1) assay, showing

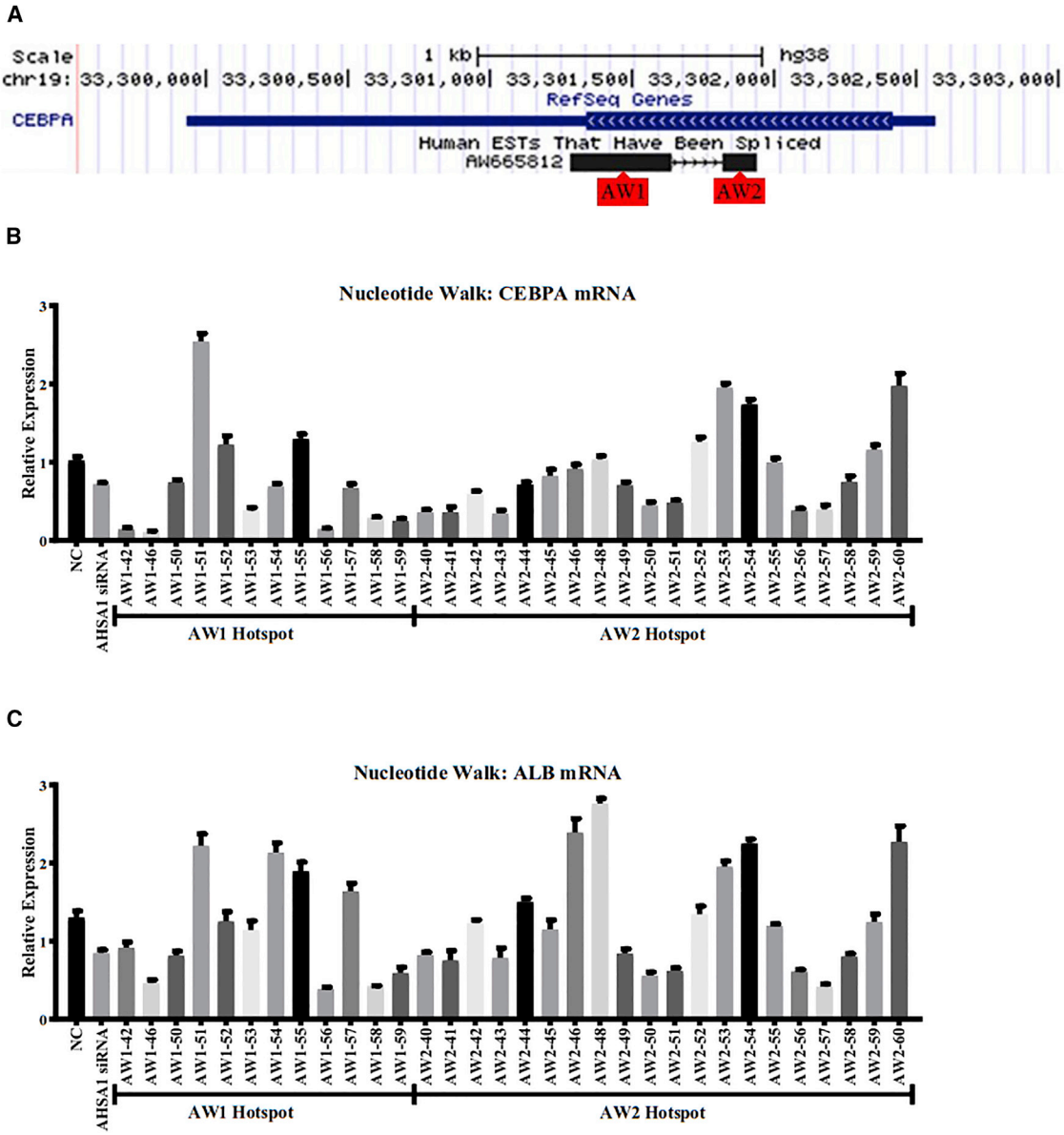

Figure 1. Nucleotide Walk on CEBPA saRNA Hotspots in HepG2 Cells

(A) Schematic showing location and orientation of CEBPA mRNA and antisense transcript GenBank: AW665812, with approximate locations of AW1 and AW2 hotspots. (B) Expression of CEBPA mRNA for each sequence transfected at 50 nM relative to mock transfected cells. (C) Expression of albumin mRNA for each sequence transfected at 50 nM relative to mock transfected cells. Error bars represent SEM.

a significant reduction in proliferation in both cell lines over a 96-hr time course (Figure 3C). Because CEBPA-51 has a canonical siRNA duplex structure, we used a bioinformatic analysis to determine if there are any predicted siRNA-like off-target effects from each strand of the CEBPA-51 duplex in the human, mouse, rat, and rhesus and cynomolgus monkey transcriptomes, as well as miRNA-like off-target effects from seed region base pairing. There were no transcripts with 0 mismatches or 1 mismatch to the AS in any of the analyzed species, and a single transcript with 1 mismatch to the SS in humans (Figure S3A). Of the 12 transcripts with 1 mismatch or 2 mismatches to either strand, we tested 6 that had known functions in liver or cancer biology for siRNA-like off-target effects. CEBPA-51 caused no significant reduction in any of these genes (Figure S3B), indicating that there is likely no off-target regulation responsible for CEBPA-51 activity consistent with the target cleavage mutation data above. The CEBPA-51 target sequence is conserved in human, non-human primates, and rodents (Figure S4A). We tested and confirmed activation of CEBPA mRNA by CEBPA-51 in CYNOM-K1 cynomolgus

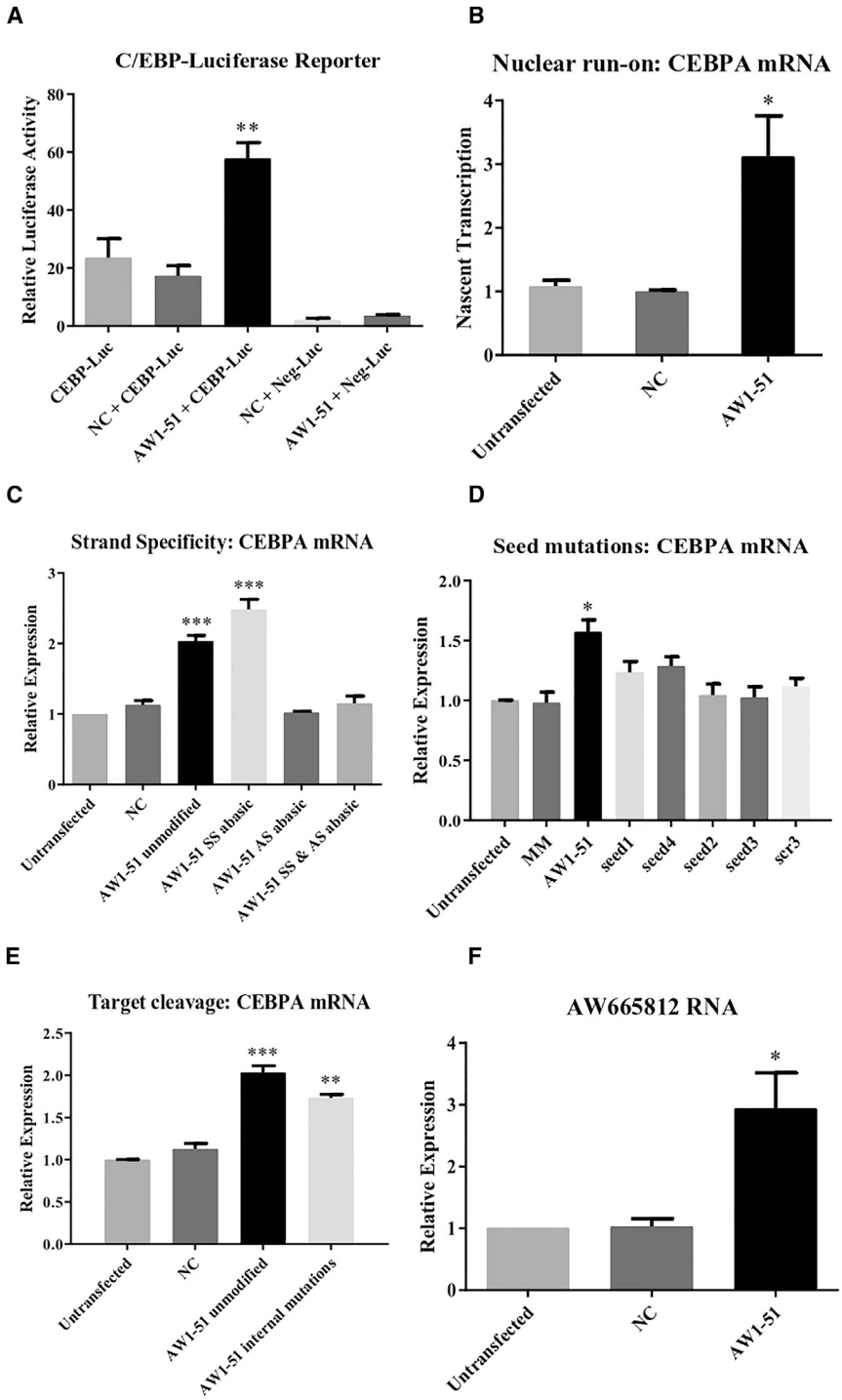

Figure 2. Mechanism of Action of AW1-51 saRNA in HepG2 Cells

(A) Relative luciferase activity representing C/EBP protein activity after transfection with 10 nM AW1-51 saRNA. (B) qPCR for CEBPA mRNA on nascent transcripts isolated from nuclear run-on after 10 nM AW1-51 saRNA transfection. (C) qPCR for CEBPA mRNA after transfection with 10 nM AW1-51 duplexes with a 5′ inverted abasic modification on the indicated strand. (D) qPCR for CEBPA mRNA after transfection with 10 nM AW1-51 saRNA with mutations in the seed region. (E) qPCR for CEBPA mRNA after transfection with 10 nM AW1-51 saRNA with mutations in the center of the duplex. (F) qPCR for GenBank: AW665812 RNA after transfection with 10 nM AW1-51. Statistical significance shown for the indicated condition compared to NC transfection: *$p < 0.05$; **$p < 0.01$; ***$p < 0.001$. Error bars represent SEM.

monkey fibroblasts and mouse embryonic fibroblasts (MEFs) (Figure S4B).

We used 3′ biotinylated SS or AS CEBPA-51 duplexes to assess the association of CEBPA-51 with Ago1–4. After transfection with 20 nM biotinylated CEBPA-51, cells were lysed and saRNA-protein complexes were purified on streptavidin beads. Subsequent western blotting showed an association of Ago2, but not Ago1, Ago3, and Ago4, to both the SS and AS strand of CEBPA-51, but not a biotinylated control oligo (Figure 4A). The importance of Ago2 for saRNA activity was confirmed by transfection of CEBPA-51 into Ago2 knockout mouse embryonic fibroblasts, where no CEBPA mRNA activation was seen. In contrast, in wild-type MEFs, a 2.3-fold activation was seen (Figure 4B). The Ago2 knockout MEFs are also negative for siRNA activity (Figure S5). We next used the biotinylated CEBPA-51 to isolate chromatin associated with CEBPA-51 after transfection. Subsequent qPCR showed a strong signal over background at the approximate genomic location of the CEBPA-51 sequence (+3 kb downstream of the transcription start site [TSS]), but not close to the TSS (Figure 4C), providing further evidence that CEBPA-51 activates CEBPA through an on-target Ago2-mediated mechanism localized to the CEBPA genomic locus. There was also no localization of CEBPA-51 at the albumin promoter (Figure 4C), and a control biotinylated oligonucleotide showed no association at the CEBPA or albumin promoters. Finally, we investigated whether activation of CEBPA mRNA by CEBPA-51 requires CTR9, a protein which has been recently shown to be part of the saRNA-induced transcriptional activation complex.[13] Co-transfection of CEBPA-51 and CTR9 siRNA abolished saRNA activity, whereas co-transfection with a negative control oligo had no effect on activity (Figure 4D), providing further evidence of an saRNA mechanism.

DISCUSSION

The field of oligonucleotide therapeutics has primarily centered around the approach of target knockdown and inhibition. The development of siRNA, antisense oligonucleotides, and microRNA mimics has provided valuable treatment options to downregulate the expression of genes involved in disease progression,[29] but there remain few options for specific upregulation of gene expression in vivo without the delivery of long synthetic mRNAs or complicated gene expression vectors. We believe that saRNAs can provide a solution for diseases where upregulation of gene expression is therapeutically beneficial, and have described here the first saRNA therapeutic to reach the clinic, CEBPA-51.

We have shown how the CEBPA-51 sequence was determined through a nucleotide walk of bioinformatically identified hotspots at the CEBPA gene. The identified saRNA, AW1-51, shows a specific dose-dependent upregulation of CEBPA mRNA, leading to an increase in functional C/EBP protein and albumin, a downstream target. This upregulation of CEBPA mRNA is from transcription of nascent mRNA, not stabilization of existing mRNA. We have also shown that this upregulation is an on-target, Ago2-mediated mechanism. Ago2 knockout cells have no CEBPA saRNA nor siRNA activity, and biotinylated CEBPA-51 saRNAs interact with Ago2 and at the expected target site 3 kb downstream of the CEBPA TSS. Interestingly, the biotinylated FLUC negative control oligo showed no association with Ago2, despite having a canonical siRNA structure. Although designed to target firefly luciferase mRNA, this duplex has been found to have no activity in cells expressing firefly luciferase (data not shown). The lack of association with Ago proteins here may be due to inefficient Ago loading or having no mRNA target in the cells 72 hr after transfection. Biotinylated CEBPA-51 was not found localized to the albumin promoter, indicating that the upregulation of albumin seen is due to C/EBP-α, not a direct interaction of the saRNA. An investigation of possible siRNA- or miRNA-like off-target effects was negative. Mutations to the seed region of the guide strand lower or negate saRNA activity, providing more evidence of an on-target sequence-dependent Ago2-mediated mechanism. However, this mechanism does not require target cleavage because cleavage-impaired AW1-51 retains activity, and the ncRNA GenBank: AW665812, despite being perfectly complementary to the AS of the saRNA, is upregulated, not downregulated, after saRNA transfection. The upregulation of this ncRNA seen here may be a general consequence of increased transcriptional activity at the CEBPA locus or it may be a regulatory component of CEBPA expression. The role of GenBank: AW665812 in CEBPA transcription is unclear and is an area of active investigation. The passenger strand of AW1-51 is also perfectly complementary to CEBPA mRNA, meaning it is possible for this duplex to act as an siRNA. The absence of any CEBPA mRNA downregulation by AW1-51 is likely due to lower internal stability of the duplex at the 5′ guide end of duplex.[30] The addition of a 5′ inverted abasic modification to the passenger strand of AW1-51 to block Ago2 loading[27] increased CEBPA mRNA upregulation, suggesting that there is passenger strand loading from the unmodified AW1-51 duplex. Future saRNA screens should include passenger strand abasic modifications to prevent loading and possible off-target effects. A previous study of the molecular mechanism of RNAa identified CTR9, a component of the PAF1 complex, to be an Ago2-associated cofactor required for saRNA activity.[13] The PAF1 complex is a known regulator of transcription and histone modification.[31] Because CEBPA-51 activity also requires CTR9, these results are consistent with previously published saRNA reports and show that the activity of CEBPA-51 is a transcriptionally driven RNAa mechanism distinct from RNAi.

The activity of CEBPA-51 has been confirmed here in two human HCC lines, where it upregulates CEBPA mRNA and protein, upregulates the downstream C/EBP-α target albumin, and inhibits cell growth. We previously showed that CEBPA saRNA also inhibits tumor growth in a rat HCC model, upregulates a range of tumor suppressor genes, and downregulates a number of oncogenic genes, such as MYC and STAT3.[11] The data reported here are consistent with this publication, and upregulation of CEBPA mRNA by CEBPA-51 is conserved in rodents and non-human primates. The modifications on CEBPA-51 prevent immune stimulation, providing evidence that the saRNA activity is not a result of innate immune reaction, and increasing the safety profile for the clinic. Similar 2′-O-methyl modification of RNA has been shown previously to suppress immune stimulation of siRNA,[32] consistent with the data reported here for saRNA.

Although surgical resection provides the best prognosis for long-term survival in HCC, many patients are ineligible for treatment due to poor liver function. We believe that upregulation of CEBPA can not only inhibit tumor cell growth as shown here, but also restore critical liver function in patients with advanced HCC. This is supported by our rat HCC model, showing reduction of tumor burden as well as increased serum albumin and decreased bilirubin, AST, and ALT with CEBPA saRNA delivery. The combination of this novel approach with already well-established oligonucleotide delivery vehicles like the NOV340 SMARTICLES[33,34] puts saRNA therapy in a unique position for translation to the clinic. This first saRNA therapeutic, CEBPA-51 encapsulated in the NOV340 SMARTICLES (MTL-CEBPA), is currently in clinical trials for patients with liver cancer.[26]

MATERIALS AND METHODS

Design of saRNA Oligonucleotides

Candidate saRNA hotspots were generated using the previously described bioinformatics algorithm.[7] The list of oligonucleotides used in this study can be found in Table S1. All bases are RNA, except when preceded by the following to indicate a modified base: m, 2′-O-methyl; d, DNA base; and ps, phosphorothioate. Nontargeting oligo "NC" or "MM" were used as a negative transfection control for experiments using unmodified saRNAs. An inactive siRNA targeting firefly luciferase ("FLUC") was used as a negative transfection control for experiments using modified saRNAs. saRNAs with seed mutations relative to AW1-51 have their changed bases underlined. Biotinylated oligos were synthesized with a biotin-triethyleneglycol (TEG) spacer attached to the 3′ end of the indicated strand of the duplex.

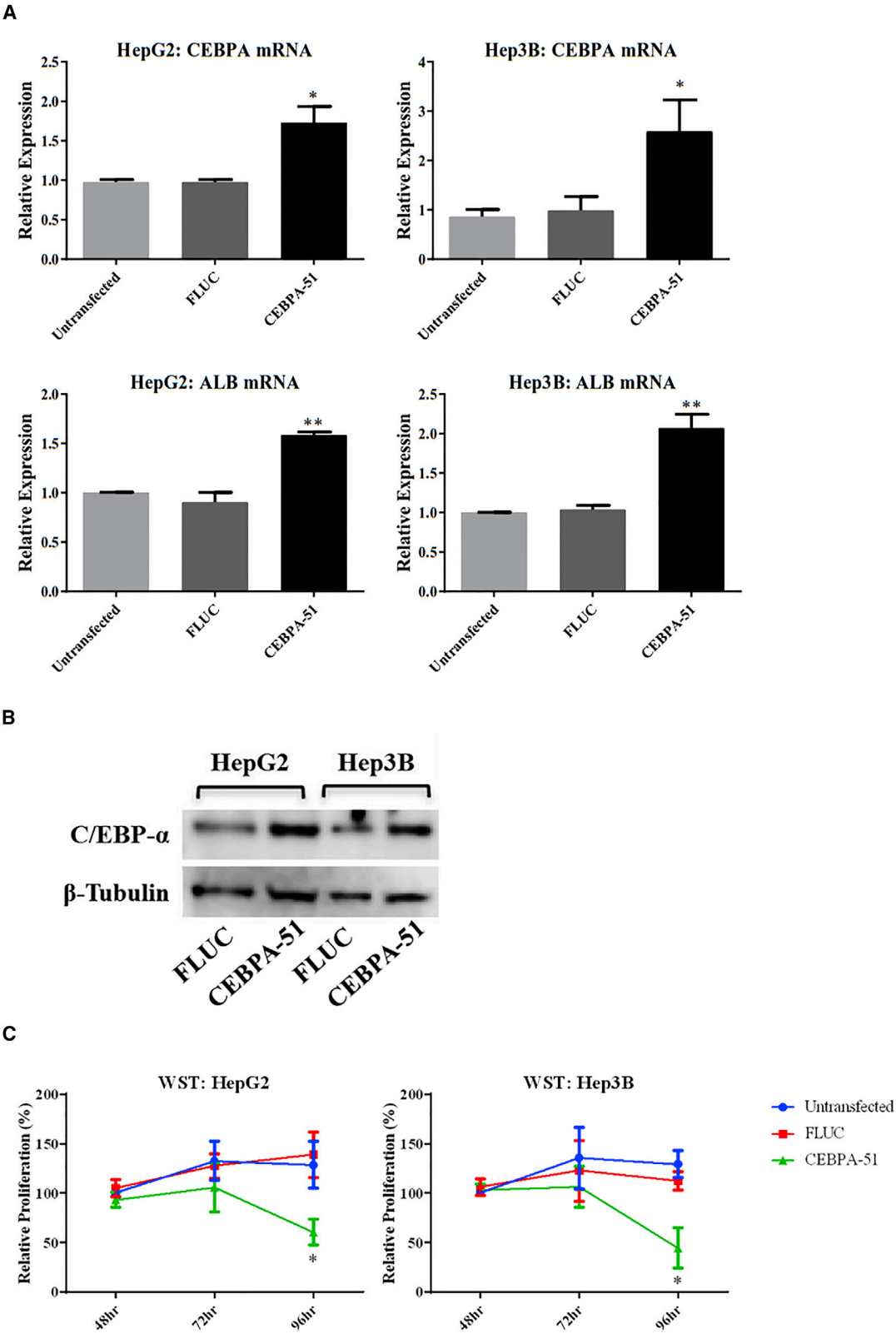

(legend on next page)

Cell Culture and Transfection

HepG2 human hepatocellular carcinoma cells (ATCC) were grown in RPMI supplemented with 10% fetal bovine serum (FBS), 2 mM L-glutamine, and penicillin/streptomycin in a 5% CO_2 incubator. Ago2 knockout mouse embryonic fibroblasts were a kind gift from Pal Saetrom. Unless otherwise specified, for transfections, the cells were seeded at 1×10^5 cells per well in a 24-well plate and reverse transfected immediately after seeding with the indicated oligonucleotide concentration using 1 μL of Lipofectamine 2000 (Life Technologies). Cells were then forward transfected after 24 hr and collected for analysis 72 hr after seeding. The indicated Silencer Negative Control (Life Technologies) or CTR9 siRNA (Life Technologies) were used for siRNA transfections.

Luciferase Assay

HepG2 cells were transfected as indicated above with the Cignal C/EBP Luciferase Reporter kit (QIAGEN) according to the manufacturer's protocol. Reporter plasmids were co-transfected with the indicated oligonucleotide at the reverse and forward transfection. After 72 hr, the cells were lysed with Passive Lysis Buffer and assayed for luciferase activity using the Dual-Luciferase Reporter Assay System (Promega) on a PHERAstar Plus luminescence microplate reader (BMG Labtech). C/EBP firefly luciferase activity was normalized to renilla luciferase activity.

Nuclear Run-On

CEBPA transcriptional activity was measured by nuclear run-on as previously described.[35] HepG2 cells were used to determine transcriptional activity after transfection with the indicated oligonucleotide.

RNA Isolation and qPCR

RNA was isolated from cultured cells using the RNeasy Mini Kit (QIAGEN). RNA was quantitated using a Nanodrop 1000 spectrophotometer (Thermo Scientific), and 500 ng was reverse transcribed using the Quantitect Reverse Transcription Kit (QIAGEN). Relative expression levels were determined by qPCR using Quantifast SYBR Green Master Mix (QIAGEN) on an ABI 7900HT thermal cycler (Applied Biosystems). The following Quantitect Primer Assays (QIAGEN) were used: ALB_1_SG, CEBPA_1_SG, CTR9_1_SG, and GAPDH_1_SG. For relative GenBank: AW665812 transcript expression, strand-specific RT primer 5′-caagaagtcggtggacaagaa was used with the Quantitect Reverse Transcription Kit before amplification with the following primers: F, 5′-cgcagcgtgtccagttc; and R, 5′-gtggagacgcagcagaag. Relative expression was determined using the ΔΔCt method normalized to GAPDH expression.

Western Blot

Cells were harvested in a 24-well-plate format (in triplicates) for a pool of 3 wells per condition for total protein extraction. Prior to cell lysis, the wells are washed twice with cold PBS and transferred into pre-chilled tubes with the use of a cell scraper. The cells were pelleted gently at 3,500 rpm for 5 min at 4°C before addition of RIPA lysis buffer containing 50 mM Tris, 150 mM NaCl, 0.1% SDS, 0.5% deoxycholate, 1% NP40, and protease inhibitor cocktail (Sigma). Cells were incubated for 10 min on ice, followed by vortexing for 2 min to allow complete cell lysis. Cell debris was then removed by centrifugation at 10,000 rpm for 10 min at 4°C. The protein supernatant was then transferred into a clean pre-chilled tube. Protein amount per sample was quantified using the RC-DC Bradford assay kit following the manufacturer's protocol (Bio-Rad), and 50 μg of total protein was loaded for SDS-PAGE. The acrylamide gels were then transferred onto polyvinylidene fluoride (PVDF) membranes for western blotting using the following antibodies: C/EBP-α, ab40764 (Abcam); β-tubulin, ab6046 (Abcam); and anti-rabbit-HRP, 926-8011 (LI-COR).

WST-1 Growth Assays

Cells were assessed for cell metabolism using the WST-1 assay, as previously described.[11] Cells were seeded at 10,000 cells per well in a 96-well plate in triplicate and transfected as described above.

Argonaute Protein Coimmunoprecipitation

HepG2 cells were seeded in 6-well plates and transfected as described above. After 72 hr, cells were cross linked with 1% formaldehyde for 15 min at 37°C in 5% incubator. Cold PBS with glycine was used to quench the formaldehyde and rinse the cells before harvest for whole cell extraction on ice using RIPA lysis buffer. Biotinylated-saRNA protein complex was immobilized using Dynabeads-Biotin Binder (Invitrogen). Following the appropriate wash cycles on a magnetic column, the eluted protein complex was then coimmunoprecipitated with anti-Ago1 (Millipore 07-599); Ago2 (Millipore 07-590); Ago3 (Abcam ab154844); or Ago4 (Abcam, ab85077). Isotype immunoglobulin G (IgG) (Santa Cruz sc0-2027) was used as a negative control. The coimmunoprecipitation complex was then immobilized using Dynabead Protein G (Thermo Fisher), and after the appropriate wash cycles on a magnetic column, samples were separated on SDS-PAGE and transferred onto a PVDF membrane for western blotting, as described above.

Chromatin Immunoprecipitation

HepG2 cells were transfected as described above. Prior to harvest, the cells were cross-linked in situ with 1% formaldehyde at 37°C for 10 min. Glycine was then added to a final concentration of 250 mM for 3 min to allow quenching of formaldehyde. Cells were washed immediately 3x with ice-cold PBS and lysed with standard RIPA lysis buffer (150 mM NaCl, 1.0% NP40, 0.5% sodium deoxycholate, 0.1% SDS, and 50 mM Tris) with 1×10^6 cells for each pull-down column. Cells were allowed to swell on ice for 10 min before chromosomal fragmentation by sonication (5x pulsed at 25%

Figure 3. Activity of CEBPA-51 in the HCC Lines HepG2 and Hep3B

(A) qPCR for CEBPA and ALB mRNA after transfection with 10 nM CEBPA-51. (B) Western blot for C/EBP-α after transfection with 10 nM CEBPA-51. (C) WST-1 assays over a 96-hr time course after transfection with 10 nM CEBPA-51. Statistical significance shown for CEBPA-51 compared to FLUC transfection: *$p < 0.05$; **$p < 0.01$. Error bars represent SEM.

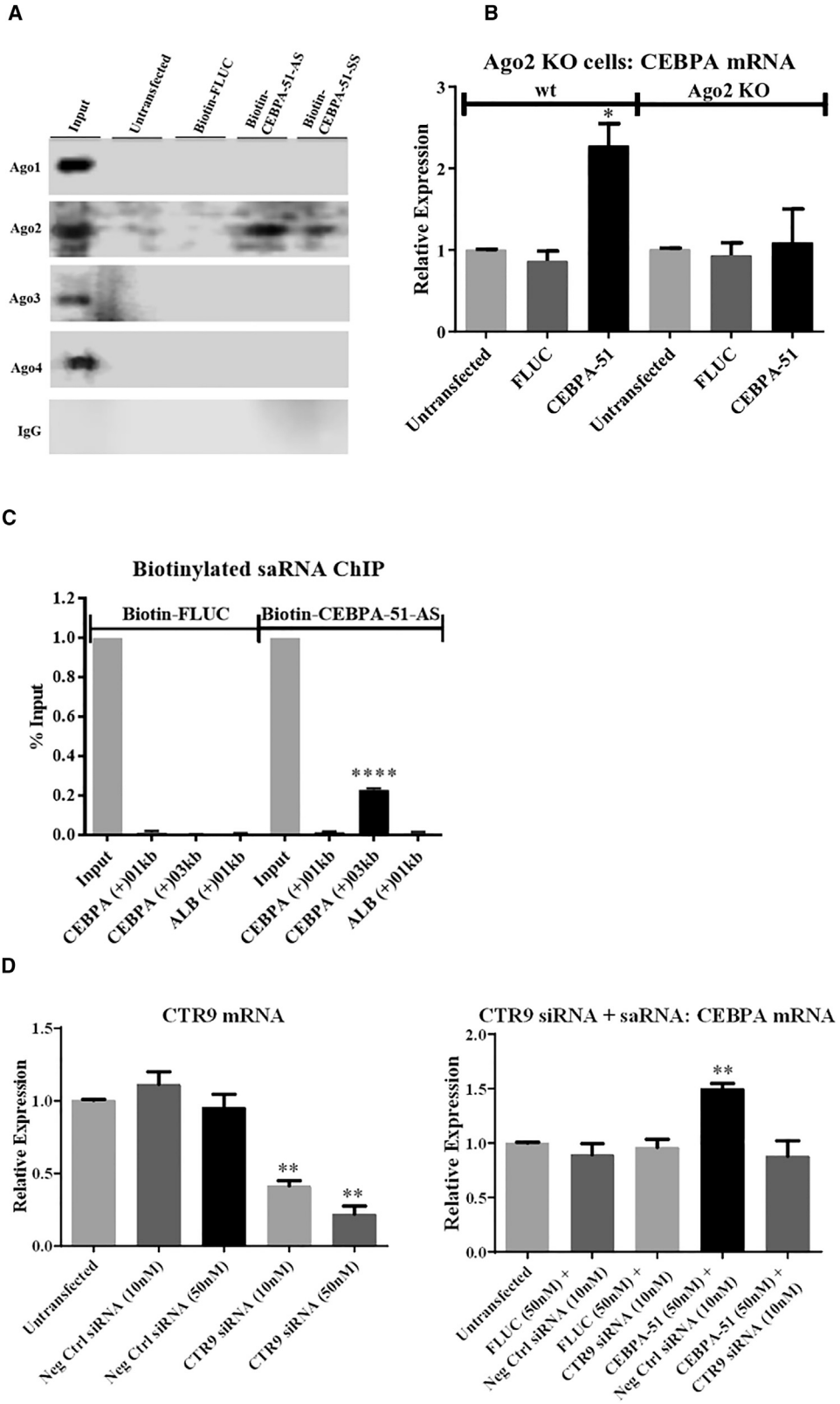

(legend on next page)

output on a Mircoson-Ultrasonic Cell disruptor XL). Cell fragments were pelleted and discarded, and the supernatant containing the fragmented chromosome was collected. Biotin immobilization was performed overnight on a rotating chamber at 4°C using a magnetic Dyna Bead Biotin Binder (Invitrogen), with the samples diluted in ChIP dilution buffer (1% SDS, 10 mM EDTA, and 50 mM Tris-HCl). The beads were then washed 2x with low salt buffer (0.1% SDS, 1% Triton X-100, 2 mM EDTA, 20 mM Tris-HCl, and 150 mM NaCl2), followed by 1x wash with high salt buffer (0.1% SDS, 1% Triton X-100, 2 mM EDTA, 20 mM Tris-HCl, and 500 mM NaCl), followed by 1x wash in lithium chloride buffer (0.25 M LiCl, 1% NP40, 1% deoxycholate, 1 mM EDTA, and 10 mM Tris-HCl), and a final 2x wash in Tris-EDTA (TE) buffer (10 mM Tris-HCl and 1 mM EDTA). The biotin/saRNA complexes were then reverse cross-linked for 4 hr at 65°C with 300 mM NaCl. DNA was then purified using phenol/chloroform/isoamyl alcohol (IAA) extraction. The DNA was precipitated in 3 M sodium acetate buffer at −80°C for at least 1 hr, followed by ultracentrifugation at 4°C. The pellet was then washed with 70% ethanol, allowed to dry, and resuspended in EB buffer for amplification using RT^2 SYBR Green qPCR Mastermix (QIAGEN), according to the manufacturer's protocol, with the following EpiTect ChIP qPCR Assays (QIAGEN): CEBPA, GPH1020591(+)01A and GPH1020591(+)03A; and ALB, GPH1010055(+)01A.

Statistical Analysis

Data are displayed as the mean of triplicates ± SEM. Statistical analysis was determined using an unpaired t test, with two-tailed p values less than 0.05 considered significant.

SUPPLEMENTAL INFORMATION

Supplemental Information includes Supplemental Materials and Methods, five figures, and one table and can be found with this article online at http://dx.doi.org/10.1016/j.ymthe.2017.07.018.

AUTHOR CONTRIBUTIONS

J.V., V.R., D.C.B., R.H., H.H., P.S., J.J.R., and N.A.H. conceptualized the study and designed experiments. P.S. designed the activating oligonucleotides. T.C.R. designed, performed, and analyzed the nuclear run-on experiments. J.V. and V.R. performed and analyzed the remaining experiments. P.P. and P.A. performed additional experiments for manuscript revision. J.V., V.R., D.C.B., R.H., and N.A.H. contributed to construction and writing of the manuscript. D.C.B., R.H., and N.A.H. managed the execution of the study.

CONFLICTS OF INTEREST

V.R., P.S., J.J.R., and N.A.H. are shareholders of MiNA (Holdings) Limited.

ACKNOWLEDGMENTS

Work was funded by MiNA Therapeutics Limited.

REFERENCES

1. Li, L.C., Okino, S.T., Zhao, H., Pookot, D., Place, R.F., Urakami, S., Enokida, H., and Dahiya, R. (2006). Small dsRNAs induce transcriptional activation in human cells. Proc. Natl. Acad. Sci. USA *103*, 17337–17342.
2. Janowski, B.A., Younger, S.T., Hardy, D.B., Ram, R., Huffman, K.E., and Corey, D.R. (2007). Activating gene expression in mammalian cells with promoter-targeted duplex RNAs. Nat. Chem. Biol. *3*, 166–173.
3. Turunen, M.P., Lehtola, T., Heinonen, S.E., Assefa, G.S., Korpisalo, P., Girnary, R., Glass, C.K., Väisänen, S., and Ylä-Herttuala, S. (2009). Efficient regulation of VEGF expression by promoter-targeted lentiviral shRNAs based on epigenetic mechanism: a novel example of epigenetherapy. Circ. Res. *105*, 604–609.
4. Chu, Y., Yue, X., Younger, S.T., Janowski, B.A., and Corey, D.R. (2010). Involvement of argonaute proteins in gene silencing and activation by RNAs complementary to a non-coding transcript at the progesterone receptor promoter. Nucleic Acids Res. *38*, 7736–7748.
5. Huang, V., Qin, Y., Wang, J., Wang, X., Place, R.F., Lin, G., Lue, T.F., and Li, L.C. (2010). RNAa is conserved in mammalian cells. PLoS ONE *5*, e8848.
6. Wang, J., Place, R.F., Huang, V., Wang, X., Noonan, E.J., Magyar, C.E., Huang, J., and Li, L.C. (2010). Prognostic value and function of KLF4 in prostate cancer: RNAa and vector-mediated overexpression identify KLF4 as an inhibitor of tumor cell growth and migration. Cancer Res. *70*, 10182–10191.
7. Voutila, J., Sætrom, P., Mintz, P., Sun, G., Alluin, J., Rossi, J.J., Habib, N.A., and Kasahara, N. (2012). Gene expression profile changes after short-activating RNA-mediated induction of endogenous pluripotency factors in human mesenchymal stem cells. Mol. Ther. Nucleic Acids *1*, e35.
8. Wang, X., Wang, J., Huang, V., Place, R.F., and Li, L.C. (2012). Induction of NANOG expression by targeting promoter sequence with small activating RNA antagonizes retinoic acid-induced differentiation. Biochem. J. *443*, 821–828.
9. Wang, T., Li, M., Yuan, H., Zhan, Y., Xu, H., Wang, S., Yang, W., Liu, J., Ye, Z., and Li, L.C. (2013). saRNA guided iNOS up-regulation improves erectile function of diabetic rats. J. Urol. *190*, 790–798.
10. Reebye, V., Saetrom, P., Mintz, P.J., Rossi, J.J., Kasahara, N., Nteliopoulos, G., Nicholls, J., Haoudi, A., Gordon, M., and Habib, N.A. (2013). A short-activating RNA oligonucleotide targeting the islet β-cell transcriptional factor MafA in CD34(+) cells. Mol. Ther. Nucleic Acids *2*, e97.
11. Reebye, V., Sætrom, P., Mintz, P.J., Huang, K.W., Swiderski, P., Peng, L., Liu, C., Liu, X., Lindkaer-Jensen, S., Zacharoulis, D., et al. (2014). Novel RNA oligonucleotide improves liver function and inhibits liver carcinogenesis in vivo. Hepatology *59*, 216–227.
12. Portnoy, V., Huang, V., Place, R.F., and Li, L.C. (2011). Small RNA and transcriptional upregulation. Wiley Interdiscip. Rev. RNA *2*, 748–760.
13. Portnoy, V., Lin, S.H., Li, K.H., Burlingame, A., Hu, Z.H., Li, H., and Li, L.C. (2016). saRNA-guided Ago2 targets the RITA complex to promoters to stimulate transcription. Cell Res. *26*, 320–335.
14. Perz, J.F., Armstrong, G.L., Farrington, L.A., Hutin, Y.J., and Bell, B.P. (2006). The contributions of hepatitis B virus and hepatitis C virus infections to cirrhosis and primary liver cancer worldwide. J. Hepatol. *45*, 529–538.
15. White, D.L., Kanwal, F., and El-Serag, H.B. (2012). Association between nonalcoholic fatty liver disease and risk for hepatocellular cancer, based on systematic review. Clin. Gastroenterol. Hepatol. *10*, 1342–1359.e2.
16. Johnson, P.J. (2005). Non-surgical treatment of hepatocellular carcinoma. HPB (Oxford) *7*, 50–55.

Figure 4. Mechanism of Action of CEBPA-51 in HepG2 Cells

(A) Western blot after co-immunoprecipitation of Ago1–4 and biotinylated CEBPA-51. (B) qPCR for CEBPA mRNA after transfection of 10 nM CEBPA-51 wild-type and Ago2 knockout MEFs. (C) qPCR at the CEBPA locus after chromatin immunoprecipitation with biotinylated CEBPA-51. The CEBPA-51 target site is approximately 3 kb downstream of the CEBPA TSS. (D) qPCR for CTR9 mRNA after transfection with CTR9 siRNA and qPCR for CEBPA mRNA after co-transfection of CTR9 siRNA and CEBPA-51. Statistical significance shown for the indicated condition compared to FLUC transfection: **p < 0.01. Error bars represent SEM.

17. Llovet, J.M., Ricci, S., Mazzaferro, V., Hilgard, P., Gane, E., Blanc, J.F., de Oliveira, A.C., Santoro, A., Raoul, J.L., Forner, A., et al.; SHARP Investigators Study Group (2008). Sorafenib in advanced hepatocellular carcinoma. N. Engl. J. Med. *359*, 378–390.

18. Ramji, D.P., and Foka, P. (2002). CCAAT/enhancer-binding proteins: structure, function and regulation. Biochem. J. *365*, 561–575.

19. Akai, Y., Oitate, T., Koike, T., and Shiojiri, N. (2014). Impaired hepatocyte maturation, abnormal expression of biliary transcription factors and liver fibrosis in C/EBPα(Cebpa)-knockout mice. Histol. Histopathol. *29*, 107–125.

20. Flodby, P., Liao, D.Z., Blanck, A., Xanthopoulos, K.G., and Hällström, I.P. (1995). Expression of the liver-enriched transcription factors C/EBP alpha, C/EBP beta, HNF-1, and HNF-4 in preneoplastic nodules and hepatocellular carcinoma in rat liver. Mol. Carcinog. *12*, 103–109.

21. Tseng, H.H., Hwang, Y.H., Yeh, K.T., Chang, J.G., Chen, Y.L., and Yu, H.S. (2009). Reduced expression of C/EBP alpha protein in hepatocellular carcinoma is associated with advanced tumor stage and shortened patient survival. J. Cancer Res. Clin. Oncol. *135*, 241–247.

22. Johnson, P.J., Berhane, S., Kagebayashi, C., Satomura, S., Teng, M., Reeves, H.L., O'Beirne, J., Fox, R., Skowronska, A., Palmer, D., et al. (2015). Assessment of liver function in patients with hepatocellular carcinoma: a new evidence-based approach-the ALBI grade. J. Clin. Oncol. *33*, 550–558.

23. Schuster, M.B., and Porse, B.T. (2006). C/EBPalpha: a tumour suppressor in multiple tissues? Biochim. Biophys. Acta *1766*, 88–103.

24. Tan, E.H., Hooi, S.C., Laban, M., Wong, E., Ponniah, S., Wee, A., and Wang, N.D. (2005). CCAAT/enhancer binding protein alpha knock-in mice exhibit early liver glycogen storage and reduced susceptibility to hepatocellular carcinoma. Cancer Res. *65*, 10330–10337.

25. Ribero, D., Curley, S.A., Imamura, H., Madoff, D.C., Nagorney, D.M., Ng, K.K., Donadon, M., Vilgrain, V., Torzilli, G., Roh, M., et al. (2008). Selection for resection of hepatocellular carcinoma and surgical strategy: indications for resection, evaluation of liver function, portal vein embolization, and resection. Ann. Surg. Oncol. *15*, 986–992.

26. ClinicalTrials.gov. (2016). First-in-human safety and tolerability study of MTL-CEBPA in patients with advanced liver cancer. https://ClinicalTrials.gov/show/NCT02716012.

27. Lima, W.F., Wu, H., Nichols, J.G., Sun, H., Murray, H.M., and Crooke, S.T. (2009). Binding and cleavage specificities of human Argonaute2. J. Biol. Chem. *284*, 26017–26028.

28. Elbashir, S.M., Martinez, J., Patkaniowska, A., Lendeckel, W., and Tuschl, T. (2001). Functional anatomy of siRNAs for mediating efficient RNAi in Drosophila melanogaster embryo lysate. EMBO J. *20*, 6877–6888.

29. Lundin, K.E., Gissberg, O., and Smith, C.I. (2015). Oligonucleotide therapies: the past and the present. Hum. Gene Ther. *26*, 475–485.

30. Khvorova, A., Reynolds, A., and Jayasena, S.D. (2003). Functional siRNAs and miRNAs exhibit strand bias. Cell *115*, 209–216.

31. Jaehning, J.A. (2010). The Paf1 complex: platform or player in RNA polymerase II transcription? Biochim. Biophys. Acta *1799*, 379–388.

32. Broering, R., Real, C.I., John, M.J., Jahn-Hofmann, K., Ickenstein, L.M., Kleinehr, K., Paul, A., Gibbert, K., Dittmer, U., Gerken, G., et al. (2014). Chemical modifications on siRNAs avoid Toll-like-receptor-mediated activation of the hepatic immune system in vivo and in vitro. Int. Immunol. *26*, 35–46.

33. Reebye, V., Voutila, J., Huang, K.-W., Muragundla, A., Jayaprakash, A., Vadnal, P., Huber, H., Habib, R., Sætrom, P., Rossi, J., et al. (2015). Systemic administration of a novel development candidate, MTL-CEBPA, up-regulates the liver-enriched transcription factor C/EBP-α and reverses CCl_4-induced liver failure in vivo. Hepatology *62* (*Suppl 1*), 269A–270A.

34. Tolcher, A.W., Rodrigueza, W.V., Rasco, D.W., Patnaik, A., Papadopoulos, K.P., Amaya, A., Moore, T.D., Gaylor, S.K., Bisgaier, C.L., Sooch, M.P., et al. (2014). A phase 1 study of the BCL2-targeted deoxyribonucleic acid inhibitor (DNAi) PNT2258 in patients with advanced solid tumors. Cancer Chemother. Pharmacol. *73*, 363–371.

35. Roberts, T.C., Hart, J.R., Kaikkonen, M.U., Weinberg, M.S., Vogt, P.K., and Morris, K.V. (2015). Quantification of nascent transcription by bromouridine immunocapture nuclear run-on RT-qPCR. Nat. Protoc. *10*, 1198–1211.

YMTHE, Volume *25*

Supplemental Information

Development and Mechanism of Small Activating RNA Targeting CEBPA, a Novel Therapeutic in Clinical Trials for Liver Cancer

Jon Voutila, Vikash Reebye, Thomas C. Roberts, Pantelitsa Protopapa, Pinelopi Andrikakou, David C. Blakey, Robert Habib, Hans Huber, Pal Saetrom, John J. Rossi, and Nagy A. Habib

Supplemental Methods

Nucleotide walk and dose response curves for CEBPA saRNAs

Transfections were performed as described in the main text. The branched DNA assay (Panomics) was used for mRNA quantification, in the version Quantigene 2.0 for target genes, and in the version Quantigene 1.0 for hsGAPDH. This hybridization-based assay system provides a chemo-luminescence readout. Probe sets were custom designed by Panomics. The assay was performed according to the manufacturer's instructions: Briefly, lysates were hybridized overnight with the respective probe set and subsequently processed for signal development. Signals were measured on a Victor Light luminescence reader (Perkin Elmer). For analysis of transfection experiments, luminescence units obtained for target mRNAs were normalized to the housekeeper mRNA GAPDH. Relative expression values obtained for transfection reagent only ("mock") treated cells were set to 1.

Isolation of human PBMCs from buffy coat of healthy donors

Peripheral blood mononuclear cells (PBMCs) were isolated by gradient centrifugation. Briefly, human buffy coat blood (obtained from Institute of Transfusion Medicine, Suhl, Germany) of three donors was fractionated by a Ficoll gradient (Sigma-Aldrich Chemie GmbH, Steinheim, Germany). The layer of white blood cells was aspirated, purified by a second gradient centrifugation and finally washed twice with cell culture medium (RPMI1640 without supplements). Viability and morphology of huPBMCs from all three donors were assessed by microscopy and PBMCs of two donors were nominated and used in subsequent experiments.

Assaying TNF-α stimulation in PBMCs

For monitoring a potential TNF-α stimulation, freshly isolated PBMCs from two healthy donors were seeded in regular 96-well tissue culture plates at a density of 100000 cells/well in 100µl complete medium (RPMI1640 supplemented with standard concentrations of L-Glutamine and 10% FCS). Cells were transfected in triplicate with 133 nM CEBPA-51 or control sequences RD-01010 (positive control) and RD-01011 (negative control) using Dotap (Roche Diagnostics, Mannheim, Germany) as a transfection reagent according to the manufacturer's protocol. Transfection reagent alone was used as mock control. In addition, controls ODN2216 (CpG-oligonucleotide) and RD-01002 (cholesterol-conjugated siRNA) were added directly at a concentration of 500nM without transfection. Cells were incubated for 20 h. Supernatants from triplicate transfections were pooled and TNF-α secretion was measured using the "Human TNF-α Instant ELISA" system (eBioscience, Frankfurt, Germany, #BMS223INSTCE), according to the manufacturer's protocol. Each sample was measured in duplicate.

Assaying IFN-α stimulation in PBMCs

For monitoring IFN-α stimulation, freshly isolated PBMCs of two healthy donors were seeded in regular 96-well tissue culture plates at a density of 100000 cells/well in 100µl complete medium (RPMI1640 supplemented with standard concentrations of L-Glutamine and 10% FCS plus

PHA-P (Phytohemagglutinin, 5µg/ml) and Interleukin-3 (10ng/ml)). Cells were transfected in triplicate with 133 nM CEBPA-51 or control sequences RD-01010 (positive control) and RD-01011 (negative control) using Geneporter-2 (Genlantis, San Diego, USA) as a transfection reagent according to the manufacturer's protocol. Transfection reagent alone was used as mock control. In addition, controls ODN2216 (CpG-oligonucleotide) and RD-01002 (cholesterol-conjugated siRNA) were added directly at a concentration of 500nM without transfection. Cells were incubated for 20 h. Supernatants from triplicate transfections were pooled and IFN-α secretion was measured using the "Human IFN-α Instant ELISA" system (eBioscience, Frankfurt, Germany, BMS216INSTCE), according to the manufacturer's protocol. Each sample was measured in duplicate.

Off-target analysis

At first potential off-target sites with full or partial complementarity to the sense and antisense strand of saRNA CEBPA51, respectively, were predicted in human, rhesus monkey, cynomolgus monkey, mouse, and rat transcriptomes (NCBI Reference Database release 69, January 2015) using a proprietary algorithm. Because positions 1 and 19 as well as the UU 3'-overhang of a siRNA are not essential for the siRNA activity only the 17mer sequence from position 2 through 18 was considered for the prediction of potential off-target sites with up to 4 mismatches to the examined saRNA strand. Based on the number and the position of the mismatches a specificity score was calculated for each predicted off-target site. The specificity score for the most likely off-target site was assigned to the corresponding saRNA strand. In addition the number of predicted off-target genes with 0, 1, 2, 3 or 4 mismatches (off-target frequency) was separately calculated for each saRNA strand.

At next potential seed-dependent, microRNA-like off-target effects were analyszed. siRNAs can function in a miRNA like manner via base-pairing of the seed-region (typically bases 2 through 7) with complementary sequences within the 3'-UTR of any mRNA molecule. In silico prediction of functional miRNA-target sites is still not well established and usually results in the prediction of thousands of potentially miRNA-regulated transcripts, which is inappropriate for the evaluation of the risk of potential microRNA-like off-target effects. Therefore we focused on seed-region sequences of known miRNAs for which it is highly likely that functional miRNA target-sites exist. This was accomplished by comparison of the seed-region (positions 2 through 7) of each saRNA strand with the seed-regions (positions 2 through 7) of known mature miRNAs from human, rhesus-monkey, rat, and mouse (miRBase release 21, June 2014). If applicable the seed-region identity and the name of the corresponding miRNA were tabulated for the sense and the antisense strand. Results are summarized in tab. 1 A and B. After that, listings with all predicted off-targets for all examined species and for both saRNA strands were created. Features of the predicted off-target sites were described in detail: strand orientation, accession number, gene ID, gene symbol, transcript description, sequence of off-target site, number and position of mismatches, location of target site (coordinates and region), indication of perfect seed match (6mer seed for position 2-7, and 7mer seed for positions 2-8). In order to allow a more refined ranking the predicted off-target sites were then further classified based on the number of mismatches, the position of the mismatches and the location of the predicted target-sites in the 5'-UTR and CDS or the 3'-UTR. The classification ranges from class 1 (most likely off-targets) to class 11 (least likely off-targets), with the most likely off-targets having no or few mismatches

and having a perfect match of the saRNA seed region with the 3‘-UTR of the predicted off-target. At next a representative transcript was defined for each off-target site in order to reduce redundancy of the potential presence of the same target-site sequence in multiple transcripts or within the same transcript. Finally the predicted off-targets were ranked according to the assigned off- target class. In the last step all predicted off-targets matched with up to 2 mismatches were listed in a separate table and identical off-targets predicted for human and at least one other species were indicated.

The cell lines Panc-1 and HuH7 were purchased from ATCC and cultured under the conditions recommended by the provider. For transfection, cells were plated directly into the transfection solution at a density of 15000 cells /well in a 96-well cell culture dish (“reverse transfection”). Lipofectamine 2000 (Life Technologies) was used as transfection reagent according to the manufacturer’s protocol. All transfections were performed in quadruplicate. The test substance CEBPA51 (XD-03934) was transfected in 3 concentrations (2 nM, 10 nM and 50 nM), scrambled control XD-03291 and Aha-1 transfection control XD-00033 were transfected at the highest concentration only. After 24h incubation, cells were lysed with 150 µl of lysis mixture (Quantigene 2.0 assay kit, Panomics) diluted 1:3 with cell culture medium. Lysates were kept frozen until analysis.

The branched DNA assay (Panomics /Affymetrix, Fremont, CA) was used for mRNA quantification, in the version Quantigene 2.0 for target genes, and in the version Quantigene 1.0 for hsGAP-DH and mmGAPDH. This hybridization-based assay system provides a chemo-luminescence readout. Probe sets were custom designed by Panomics. The assay was performed according to the manufacturer’s instructions: Briefly, lysates were hybridized over night with the respective probe set and subsequently processed for signal development. Signals were measured on a Victor Light luminescence reader (Perkin Elmer). For analysis of transfection experiments, luminescence units obtained for target mRNAs were normalized to the housekeeper mRNA for GAPDH. Relative expression values obtained for transfection reagent only (“mock”) treated cells were set to 1.

Cynomolgus cross-reactivity

CYNOM-K1 cynomolgus skin fibroblasts (Sigma) were maintained in MEM supplemented with 10% FBS, 2mM L-glutamine, and penicillin/streptomycin in a 5% CO_2 incubator. Cells were transfected with Lipofectamine 2000 as described in the main text with the indicated oligonucleotide and were harvested for analysis after 48 hours.

Supplemental Table 1

Name	SS Sequence (5’->3’)	AS Sequence (5’->3’)	Notes
NC	ACUACUGAGUGACAGUAGAUU	UCUACUGUCACUCAGUAGUUU	Unmodified non-targeting negative control
MM	UCGAAGUAUUCCGCGUACGUU	CGUACGCGGAAUACUUCGAUU	Unmodified non-targeting negative control

FLUC	mCmUmUAmCGmCmUGA GmUAmCmUmUmCGAdTpsdT	UCGAAGmUACUmU AGCGmUAAGdTpsdT	Modified FLUC negative control
AHSA1 siRNA	GGAmUGAAGmUGG AGAmUmUAGmUdTpsdT	ACmUAAUCUCmCA CUUmCAUCCdTpsdT	siRNA to AHSA1
AW1-42	GUCACUGGUCAGCUCCAGCUU	GCUGGAGCUGACCAGUGACUU	-8nt from AW1 hotspot
AW1-46	CAUUGUCACUGGUCAGCUCUU	GAGCUGACCAGUGACAAUGUU	-4nt from AW1 hotspot
AW1-50	CGGUCAUUGUCACUGGUCAUU	UGACCAGUGACAAUGACCGUU	AW1 hotspot
AW1-51	GCGGUCAUUGUCACUGGUCUU	GACCAGUGACAAUGACCGCUU	+1nt from AW1 hotspot
AW1-52	GGCGGUCAUUGUCACUGGUUU	ACCAGUGACAAUGACCGCCUU	+2nt from AW1 hotspot
AW1-53	AGGCGGUCAUUGUCACUGGUU	CCAGUGACAAUGACCGCCUUU	+3nt from AW1 hotspot
AW1-54	CAGGCGGUCAUUGUCACUGUU	CAGUGACAAUGACCGCCUGUU	+4nt from AW1 hotspot
AW1-55	GCAGGCGGUCAUUGUCACUUU	AGUGACAAUGACCGCCUGCUU	+5nt from AW1 hotspot
AW1-56	CGCAGGCGGUCAUUGUCACUU	GUGACAAUGACCGCCUGCGUU	+6nt from AW1 hotspot
AW1-57	GCGCAGGCGGUCAUUGUCAUU	UGACAAUGACCGCCUGCGCUU	+7nt from AW1 hotspot
AW1-58	UGCGCAGGCGGUCAUUGUCUU	GACAAUGACCGCCUGCGCAUU	+8nt from AW1 hotspot
AW1-59	UUGCGCAGGCGGUCAUUGUUU	ACAAUGACCGCCUGCGCAAUU	+9nt from AW1 hotspot
AW2-40	AUUCAUCCUCCUCGCGGGGUU	CCCCGCGAGGAGGAUGAAUUU	-10nt from AW2 hotspot
AW2-41	GAUUCAUCCUCCUCGCGGGUU	CCCGCGAGGAGGAUGAAUCUU	-9nt from AW2 hotspot
AW2-42	GGAUUCAUCCUCCUCGCGGUU	CCGCGAGGAGGAUGAAUCCUU	-8nt from AW2 hotspot
AW2-43	AGGAUUCAUCCUCCUCGCGUU	CGCGAGGAGGAUGAAUCCUUU	-7nt from AW2 hotspot
AW2-44	AAGGAUUCAUCCUCCUCGCUU	GCGAGGAGGAUGAAUCCUUUU	-6nt from AW2 hotspot
AW2-45	AAAGGAUUCAUCCUCCUCGUU	CGAGGAGGAUGAAUCCUUUUU	-5nt from AW2 hotspot
AW2-46	UGAAAGGAUUCAUCCUCCUUU	AGGAGGAUGAAUCCUUUCAUU	-4nt from AW2 hotspot
AW2-48	CUGAAAGGAUUCAUCCUCCUU	GGAGGAUGAAUCCUUUCAGUU	-2nt from AW2 hotspot
AW2-49	GCUGAAAGGAUUCAUCCUCUU	GAGGAUGAAUCCUUUCAGCUU	-1nt from AW2 hotspot
AW2-50	AGCUGAAAGGAUUCAUCCUUU	AGGAUGAAUCCUUUCAGCUUU	AW2 hotspot
AW2-51	CAGCUGAAAGGAUUCAUCCUU	GGAUGAAUCCUUUCAGCUGUU	+1nt from AW2 hotspot
AW2-52	CCAGCUGAAAGGAUUCAUCUU	GAUGAAUCCUUUCAGCUGGUU	+2nt from AW2 hotspot
AW2-53	GCCAGCUGAAAGGAUUCAUUU	AUGAAUCCUUUCAGCUGGCUU	+3nt from AW2 hotspot
AW2-54	CGCCAGCUGAAAGGAUUCAUU	UGAAUCCUUUCAGCUGGCGUU	+4nt from AW2 hotspot

AW2-55	GCGCCAGCUGAAAGGAUUCUU	GAAUCCUUUCAGCUGGCGCUU	+5nt from AW2 hotspot
AW2-56	AGCGCCAGCUGAAAGGAUUUU	AAUCCUUUCAGCUGGCGCUUU	+6nt from AW2 hotspot
AW2-57	CAGCGCCAGCUGAAAGGAUUU	AUCCUUUCAGCUGGCGCUGUU	+7nt from AW2 hotspot
AW2-58	CCAGCGCCAGCUGAAAGGAUU	UCCUUUCAGCUGGCGCUGGUU	+8nt from AW2 hotspot
AW2-59	GCCAGCGCCAGCUGAAAGGUU	CCUUUCAGCUGGCGCUGGCUU	+9nt from AW2 hotspot
AW2-60	GGCCAGCGCCAGCUGAAAGUU	CUUUCAGCUGGCGCUGGCCUU	+10nt from AW2 hotspot
AW1-51 seed1	GCGGUCAUUGUCACUGCUCUU	GAGCAGUGACAAUGACCGCUU	Mutation at second seed position
AW1-51 seed4	GCGGUCAUUGUCACUCGUCUU	GACGAGUGACAAUGACCGCUU	Mutation at third seed position
AW1-51 seed2	GCGGUCAUUGUCUCAGCUCUU	GAGCUGAGACAAUGACCGCUU	Three seed mutations
AW1-51 seed3	GCGGUCAUUGUGAGUCGACUU	GUCGACUCACAAUGACCGCUU	Four seed mutations
AW1-51 scr3	GGAUUGCGUCUCGGUCUCAUU	UGAGACCGAGACGCAAUCCUU	AW1-51 sequence scrambled

Supplemental Figure 1

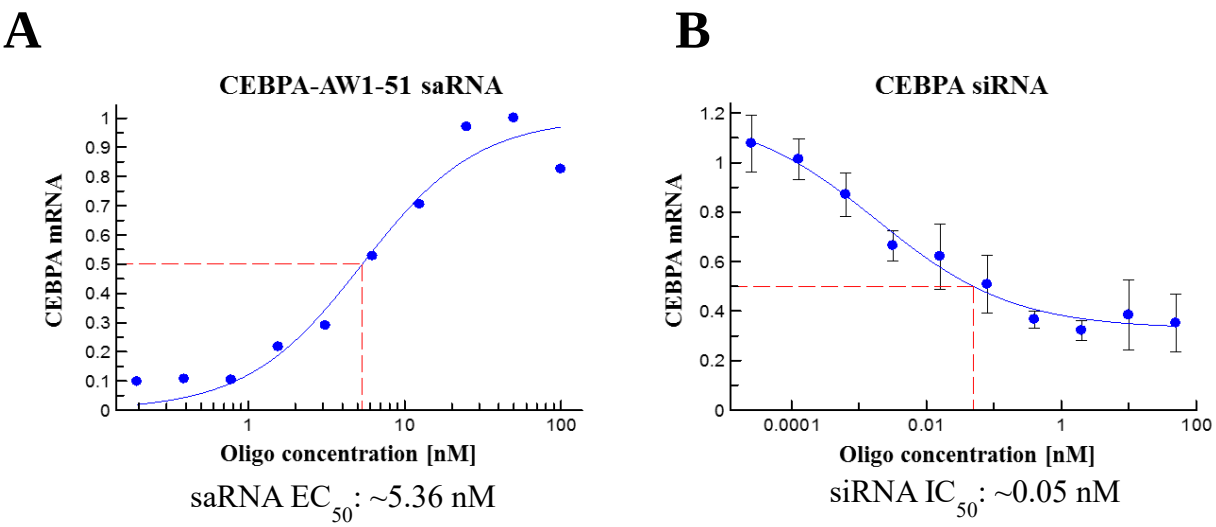

Dose response curves for CEBPA saRNA and siRNA in HepG2 cells. (A) Dose response curve for CEBPA mRNA after transfection with increasing concentrations of AW1-51 saRNA. (B) Dose response curve for CEBPA mRNA after transfection with increasing concentrations of CEBPA siRNA.

Supplemental Figure 2

A

Name	SS Sequence (5'->3')	AS Sequence (5'->3')
SS 5' inverted abasic	(invabasic)GCGGUCAUUGUCACUGGUCUU	GACCAGUGACAAUGACCGCUU
5' IA + mod pattern 1	(invabasic)GCmGGmUCmAUmUGmUCmACmUGmGUCmUmU	GACCAGUGACAAUGACCGCmUmU
5' IA + mod pattern 2	(invabasic)mGmCGmGUCAUUmGUCAmCUGGUCmUmU	GACCAGUGACAAUGACCGCmUmU
5' IA + mod pattern 3	(invabasic)mGmCGGmUmCAmUmUGmUmCAmCmUGGmUmCmUmU	GACmCAGUGAmCAAUGACCGCmUmU

B

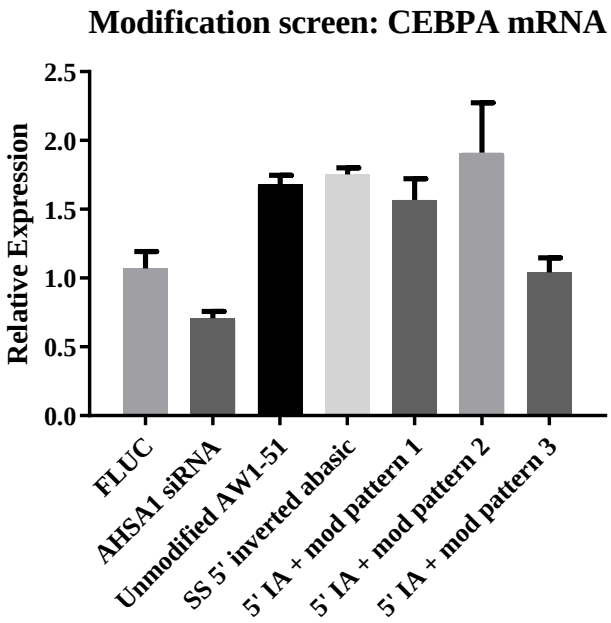

Supplemental Figure 2 (cont.)

C

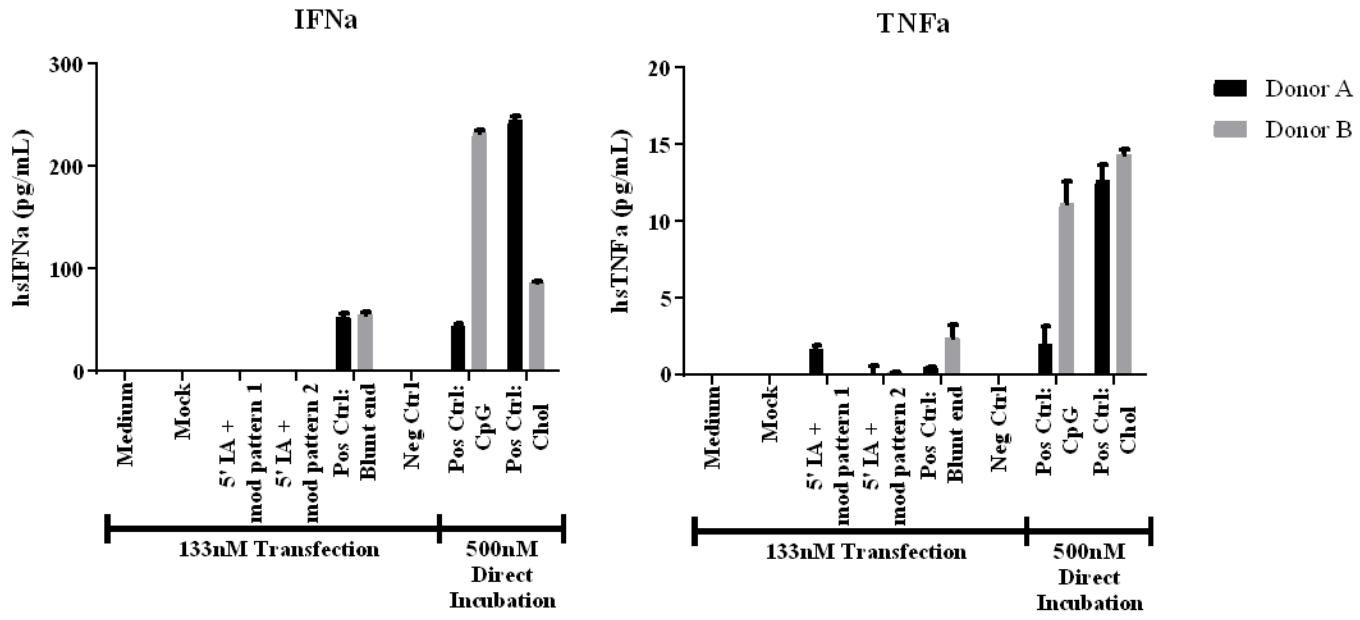

Modifications of AW1-51 to avoid immune stimulation. (A) Table showing modification patterns of AW1-51 tested. (B) qPCR for CEBPA mRNA after transfection with 10nM modified AW1-51 saRNA in HepG2 cells. (C) ELISA for TNFa and IFNa from PBMCs transfected with modified AW1-51 saRNAs.

Supplemental Figure 3

A

	antisense strand						
	miRNAs with seed regions identical to seed region of siRNA strand	Off-target frequency classified by number of mismatches					
species		score	0	1	2	3	4
human	-	3	0	0	4	79	809
rhesus monkey	-	3	0	0	2	42	534
cynomolgus monkey	n.d.	3	0	0	4	69	689
mouse	mmu-miR-470-3p, mmu-miR-1905	2	0	0	4	112	1101
rat	-	3	0	0	3	83	979

	sense strand						
	miRNAs with seed regions identical to seed region of siRNA strand	Off-target frequency classified by number of mismatches					
species		score	0	1	2	3	4
human	-	1,9	0	1	8	123	1144
rhesus monkey	-	3	0	0	5	106	876
cynomolgus monkey	n.d.	3	0	0	6	112	1074
mouse	-	2	0	0	18	170	1319
rat	-	2	0	0	18	148	1326

Supplemental Figure 3 (cont.)

B

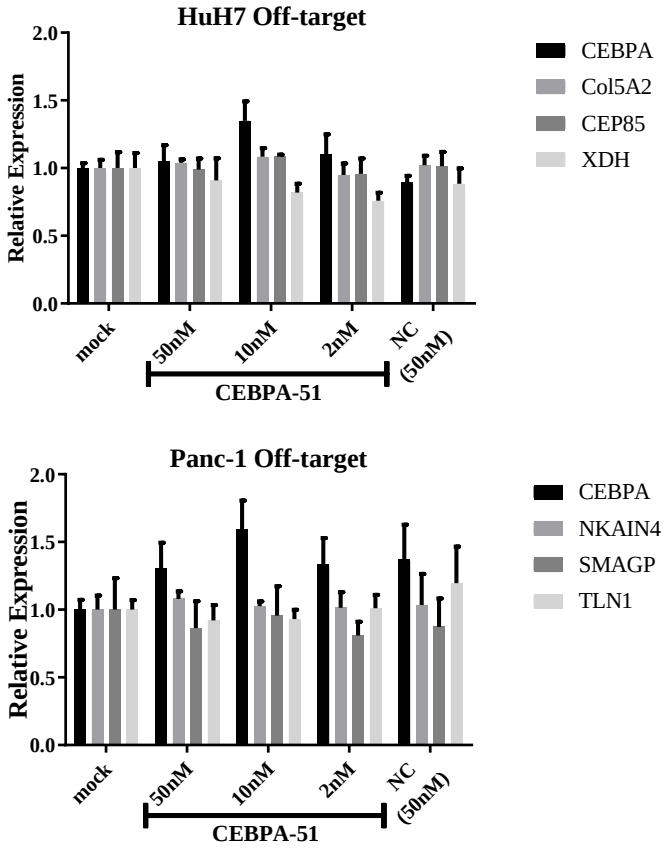

Off-target analysis of CEBPA-51 activity. (A) Table showing off-target frequency for each species analyzed. (B) Relative expression of putative off-target gene expression 24 hours after transfection with the indicated concentration of CEBPA-51.

Supplemental Figure 4

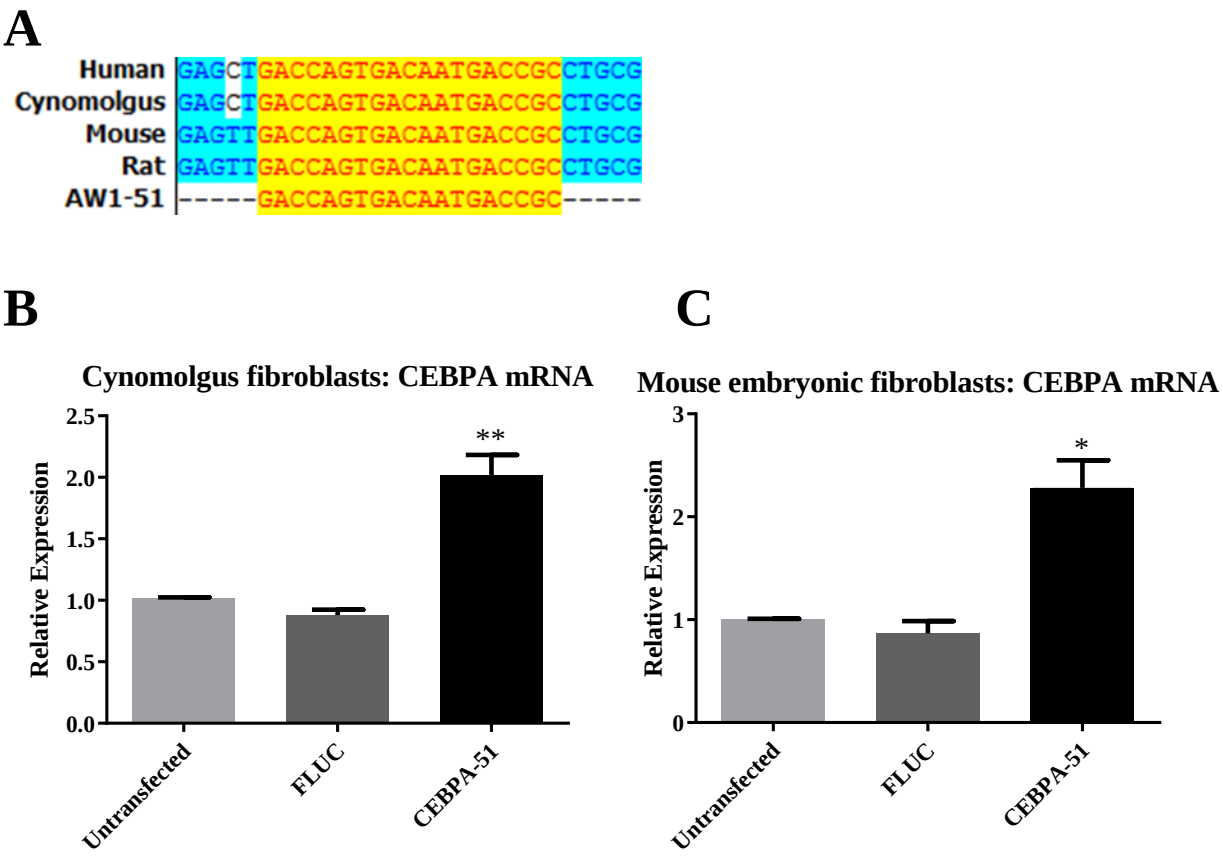

Cross-reactivity of CEBPA-51. (A) Alignment of human, cynomolgus monkey, and rodent genomic sequences at the AW1-51 target site. (B) qPCR for CEBPA mRNA after transfection of 10nM CEBPA-51 in CYNOM-K1 cells. (C) qPCR for CEBPA mRNA after transfection of 10nM CEBPA-51 in mouse embryonic fibroblasts. Statistical significance shown for CEBPA-51 compared to FLUC transfection: *, $p < 0.05$; **, $p < 0.01$.

Supplemental Figure 5

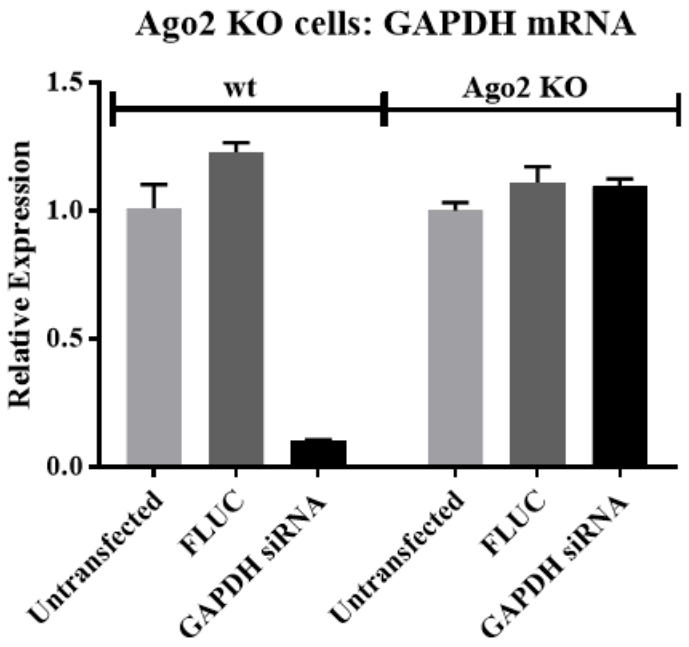

siRNA activity of Ago2 KO MEFs. Relative expression of gene expression 24 hours after transfection with control or GAPDH siRNA at 10nM.